

---

AUTOMATISED ANALYSIS OF THE TRIGGER  
TIMING FOR THE COMPASS EXPERIMENT

---

**Bachelorarbeit in Physik**

von  
Merlin Rossbach

angefertigt am  
**Physikalischen Institut der Universität Bonn**

vorgelegt der  
**Mathematisch-Naturwissenschaftlichen Fakultät**  
der  
**Rheinischen Friedrich-Wilhelms-Universität Bonn**

**Juli 2011**

Ich versichere, dass ich diese Arbeit selbständig verfasst und keine anderen als die angegebenen Quellen und Hilfsmittel benutzt sowie die Zitate kenntlich gemacht habe.

Bonn, den

Unterschrift

1. Gutachter: Prof. Dr. Hartmut Schmieden
2. Gutachter: Prof. Dr. Kai-Thomas Brinkmann

# Contents

<b>1</b>	<b>Introduction</b>	<b>4</b>
<b>2</b>	<b>COMPASS experiment</b>	<b>7</b>
2.1	Proton beam . . . . .	7
2.2	Muon beam . . . . .	7
2.3	Target . . . . .	8
2.4	Spectrometer . . . . .	8
2.5	Trigger . . . . .	9
<b>3</b>	<b>Automised determination of <math>t_0</math> offsets using <i>ROOT</i></b>	<b>12</b>
3.1	General program layout . . . . .	12
3.2	Implementation of fit . . . . .	12
<b>4</b>	<b>Results</b>	<b>15</b>
<b>5</b>	<b>Summary and outlook</b>	<b>22</b>

# 1 Introduction

In modern physics there are many open questions. Although quantum chromodynamics (QCD) has achieved a great, nearly perfect agreement of experiment and theory at high energy scales, it is not able to make good predictions in the non-perturbative region. If one regards, for example, the composition of the nucleon spin, there is still a huge lack of understanding.

When trying to understand the nucleon spin one first has to know the BJORKEN scaling variable which describes the degree of inelasticity for a scattering process and is defined as

$$x := \frac{Q^2}{2M\nu} \quad (1)$$

where  $Q$  is the four momentum,  $\nu$  the energy transfer and  $M$  the mass of the target particle. For purely elastic reactions follows  $x = 1$  and for inelastic processes  $0 < x < 1$ . The incoming particles are able to interact for instance with the substructure of the target nucleon with the radius  $R$  as shown in figure 1 if they are high energetic ( $Q^2 R^2 \gg 1$ ). When scattering an electron off the constituents of a nucleon, the BJORKEN scaling variable can be determined with  $x = \frac{1}{n} \frac{Q^2}{2M\nu}$  where  $n$  is the number of constituents. Since  $\frac{Q^2}{2M\nu}$  is 1 for elastic scattering of the electrons at the constituents of the nucleon it follows that the explanation of figure 1 where  $x = \frac{1}{3}$  is the case can be given for three constituents. The width of the resulting peak derives from the FERMI motion of the constituents which are called quarks. From the fact that the structure functions  $F_1$  and  $F_2$  do not or only weakly depend on the energy transfer  $Q^2$  one can deduce from previous results that the quarks have to be pointlike. Assuming that the quarks carry the spin of  $\frac{1}{2}$  one obtains

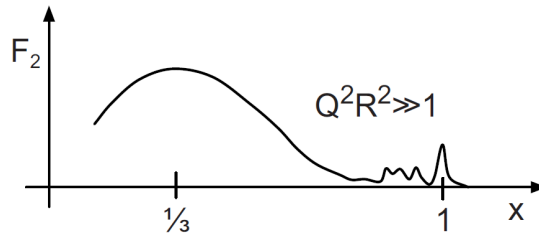


**Figure 1:** Structure function from a deep inelastic scattering process of an electron off a nucleon. The structure function is plotted for different values of the BJORKEN scaling variable. [Po09]

the CALLAN-CROSS relation

$$2xF_1(x) = F_2(x) \quad (2)$$

which has been proved experimentally. So the nucleon consists of three pointlike quarks, which all carry the spin of  $\frac{1}{2}$  (in units of  $\hbar$ ).

The naive approach to the decomposition of the nucleon spin of  $\frac{1}{2}$  would be the sum of the quarks' spin  $\Delta\Sigma$  but there are several other parts that may play a role.

$$\frac{1}{2} = \frac{1}{2}\Delta\Sigma + \Delta G + L_q + L_g \quad (3)$$

If having a closer look at the constituents of the nucleon in equation (3), the total spin of  $\frac{1}{2}$  is formed by the contribution of the quarks' spin  $\frac{1}{2}\Delta\Sigma$ , the effect of the gluon spin  $\Delta G$  and the contributions of the orbital angular momenta of quarks  $L_q$  and gluon  $L_g$ . The contribution of the quarks  $\frac{1}{2}\Delta\Sigma$  was believed to create the main part in the order of about 0.375 of the total spin  $\frac{1}{2}$ , but after some measurements of the European Muon Collaboration (EMC) it was discovered, that this part only contributes with 0.1 to 0.15 to the total spin [As88].

So it is clear that the other components need to be examined. For example one can examine

the Gluon spin contribution  $\Delta G$ . The COMPASS Collaboration decided to follow this aim by examining muon proton scattering.

In order to examine the Gluon spin contribution to the nucleon spin, one needs to tag reactions in which the partonic process involves a gluon. The virtual photon interacts with a gluon via the so called photon-gluon-fusion process (pgf)  $\gamma^* g \rightarrow c\bar{c}$ . One possibility is shown in figure 2, the muon is scattered via the exchange of a virtual photon resulting in  $c\bar{c}$  pair production. It is also possible to choose other pair productions for example  $u\bar{u}$ ,  $d\bar{d}$  or  $s\bar{s}$ , but this is impractical because the resulting particles could also be created by other mechanisms. Hence the  $c\bar{c}$  production is selected. The  $c$  and  $\bar{c}$  hadronise and produce for example  $D^0$  and  $\bar{D}^0$ .

Regarding the  $D^0$ , it decays with a branching ratio of 4% into

$$D^0 \rightarrow K^- + \pi^+ \quad (4)$$

of which both decay products can be measured.

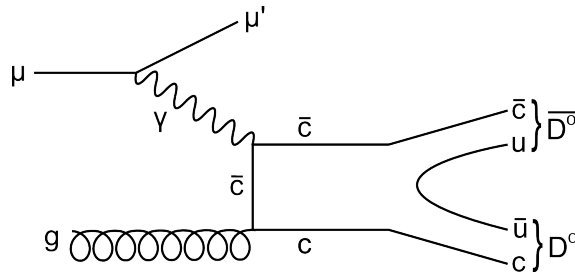


**Figure 2:** Interaction of the muon with the nucleus via the gluon and the resulting production of charmed mesons.

Out of this reaction, the polarisation of the gluon can be determined. To serve this purpose, the proton as the target particle has to be polarised. When switching the polarisation of the proton, the one of the gluon is changed as well. Measuring with different spin configurations for target and beam, it is possible to measure different cross sections for the different configurations. The double spin cross section asymmetry between target and beam polarisation is proportional to  $\frac{\Delta g}{g}$ . Therefore, it provides the information needed to calculate  $\Delta G$ .

The spin configurations of incident beam and the target have to be adjustable to make sure that the state before the collision can be determined.

The fragments of the scattering can cover a huge range of momentum and should all be measured, so it is necessary to have a large momentum acceptance.

When having measured different processes, it is very important to distinguish them by identifying the outgoing particles. Only then is it possible to examine different processes exclusively. This means that all the outgoing particles are measured. As an alternative the reaction can be identified semi-inclusive, which means that all but one outgoing particles are detected.

This leads to the prerequisites that were demanded for the COMPASS-experiment during its design:

- High energy polarised muon beam
- Polarised target
- Large momentum acceptance
- Good particle identification

During measurements at an experimental setup like COMPASS huge amounts of data accrue. Due to limited storage for data when measuring, it is mandatory that COMPASS has an effective triggering system, where each triggering signal marks an event that is worth storing.

A triggering signal is produced by two trigger hodoscopes and is shifted in time against the data

signal of one of the hodoscopes by the time interval of  $t_0$ . However it is very important to connect the data from the first hodoscope, to the whole event and therefore to the instant in time where the trigger is activated.

Hence the scope of this work is to automatise the determination of the just mentioned time difference  $t_0$  which marks the time difference between the triggering point of time and the corresponding data in the other hodoscope.

This thesis is organised as follows. The initiating overview of the COMPASS setup is followed by a closer discussion how the automatic trigger time determination was realised with the software *ROOT*. Afterwards the results of the work will be presented and discussed.

## 2 COMPASS experiment

COMPASS stands for **C**ommon **M**uon **P**roton **A**pparatus for **S**tructure and **S**pectroscopy and was built at the CERN accelerating facilities. In the following the setup of the COMPASS experiment is described.

### 2.1 Proton beam

The Super Proton Synchrotron (SPS) has been in operation since 1976 and provides the COMPASS experiment with protons that have a momentum of  $400 \frac{\text{GeV}}{c}$ . The SPS is itself fed by the Proton Synchrotron (PS) for which Proton Synchrotron Booster (PSB) and LINAC2 act as preaccelerators.

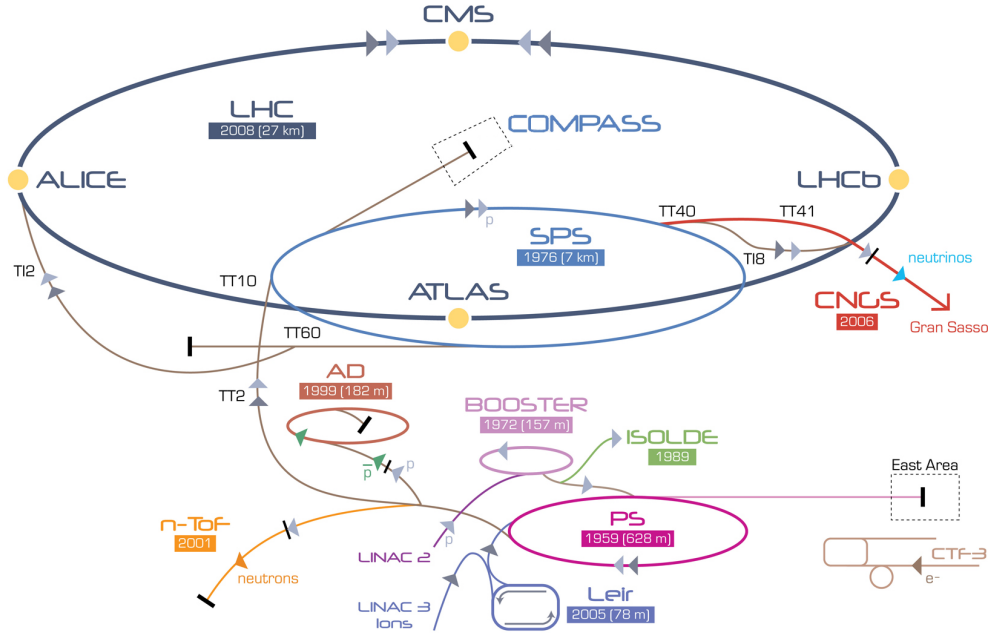


**Figure 3:** The CERN accelerators with their corresponding experiments, especially the COMPASS Experiment in the middle of LHC. [CE08]

### 2.2 Muon beam

The  $400 \frac{\text{GeV}}{c}$  protons delivered by SPS have to be transformed into a polarised and highly energetic muon beam. At first the incident proton beam is directed to a beryllium target (T6) of 50cm length (compare figure 4) and produces mainly pions and kaons of which some decay to muons. After 600m a hadron absorber ensures that only the muons can get further. To get a defined state before the collision with the COMPASS target, the produced muon beam is adjusted to a momentum of  $160 \frac{\text{GeV}}{c}$  in the Beam Momentum Station (BMS) via magnetic deflection and collimation. From there the beam is transported to the COMPASS target. As an effect of helicity conservation in weak decays, only muons with a certain helicity are allowed and thus a degree of polarisation of about 90% can be achieved when producing muons at  $160 \frac{\text{GeV}}{c}$ . So the requirement of a polarised beam is fulfilled.

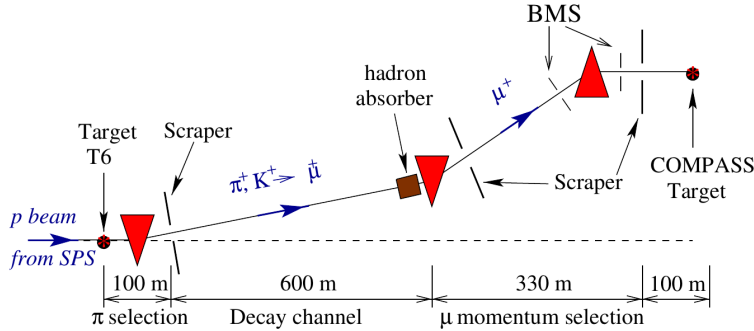


**Figure 4:** Production of muons out of incoming protons. [He09]

### 2.3 Target

As already mentioned it is required that both the used target and the beam should be polarised. To improve statistical significance of the results one has to achieve large values for the figure of merit, which is given by

$$\frac{1}{\sigma_A^2} = \left( \frac{\delta A}{A} \right)^{-2} = (P_\mu P_T f)^2 \cdot N. \quad (5)$$

It is obvious that one has to maximise the degree of polarisation of beam  $P_\mu$  and target  $P_T$  and the fraction of polarisable material in the target  $f$  since they have the main influence on the statistical significance of the experiment. Of course the second step would be to provide a high number of events  $N$ , which can only be influenced by extending the measurement time. The expected counting rate asymmetry is  $A^{raw} \propto (P_\mu P_T f)(\Delta\sigma/2\bar{\sigma})$ , where  $\Delta\sigma/2\bar{\sigma}$  is the desired cross-section asymmetry. So it is mandatory to maximise all of those three quantities  $P_\mu$ ,  $P_T$  and  $f$  to achieve the best statistic validity for the given  $N$ . For the used irradiated ammonia ( $\text{NH}_3$ ), which acts as proton target the fraction of polarisable material  $f \approx 0.15$  is slightly low but can be polarised to a high degree of  $P_T > 80\%$ .

Due to the fact that it is a solid state target, the polarisation has first to be applied to electrons from which it is transferred via dynamic nuclear polarisation (DNP). This means that the spin is transferred by a microwave field to the ammonia, requiring a strong magnetic field, a temperature below 1K and the availability of some paramagnetic centres in the target material. Those can be delivered by radiation [Ab61]. The target contains two target cells in a row, with alternating polarisation in order to directly measure the asymmetries. To keep systematical errors caused by the experimental setup low, the polarisation of all cells is switched a few times during one period of measurement.

### 2.4 Spectrometer

As the outgoing particles cover a broad momentum range, it is a design goal of the COMPASS experiment to cover a wide momentum range. This is achieved by a two stage spectrometer, each for a special angular range, to obtain maximum momentum acceptance.

It is realised via two magnets with different magnetic field strength and a large number of detectors after each of them. The first magnet provides a comparatively small bending of incident particles which is proportional to its magnetic field integral. Therefore particles with low momentum are bent measurably while particles with high momentum are barely affected. These particles can now be bent significantly by the second magnet with higher magnetic field integral. So it is possible to determine the momenta of particles via their deflection within a range of  $1 \frac{\text{GeV}}{c}$  upto almost the

beam momentum of  $160 \frac{\text{GeV}}{c}$ .

### Large angle spectrometer

The large angle spectrometer (LAS) is made to detect particles with low momentum, between 1 and  $5 \frac{\text{GeV}}{c}$ . Therefore its magnet SM1 has a low field integral of 1.0Tm. For a particle with momentum of  $1 \frac{\text{GeV}}{c}$  this would lead to a deflection of 300mrad which corresponds to approximately  $17.2^\circ$  [Ab07]. The magnet is followed by a ring imaging čerenkov (RICH) detector, which can identify charged hadrons. The LAS is completed by a hadron calorimeter (HCAL1) for detection of hadrons and a muonfilter to shield all particles but muons. Behind the muonfilter, the tracks of the particles which now must be muons can be determined with the help of the trigger hodoscopes. From the measured bending, the muon's momentum can be calculated.

### Small angle spectrometer

The second stage of the spectrometer is the small angle spectrometer (SAS) for detection of particles with momenta above  $5 \frac{\text{GeV}}{c}$ . The central component is the 4m long magnet SM2 with a integrated field of 4.4Tm. Furthermore the SAS contains an electromagnetic calorimeter (ECAL2) for detecting photons and neutral pions as well as the hadron calorimeter (HCAL2) which is used for triggering purposes. The SAS is completed by a second muonfilter and some trigger hodoscopes.

## 2.5 Trigger

Considering that COMPASS contains about 300 detector-layers it is impractical to store all events with the Data Acquisition (DAQ). Each event requires about 35kB when storing it on harddisk. For  $2 \cdot 10^8$  muons per spill around every 20s this would lead to a large amount of data [He09]. In order to prevent this the COMPASS experiment has a triggersystem that reduces the amount of data by selection of only those events that are candidates for significant events. This decreases the number of stored events to  $10^4$  per spill [Pr07]. The trigger concept is described in detail in the COMPASS triggerpaper [Be05].

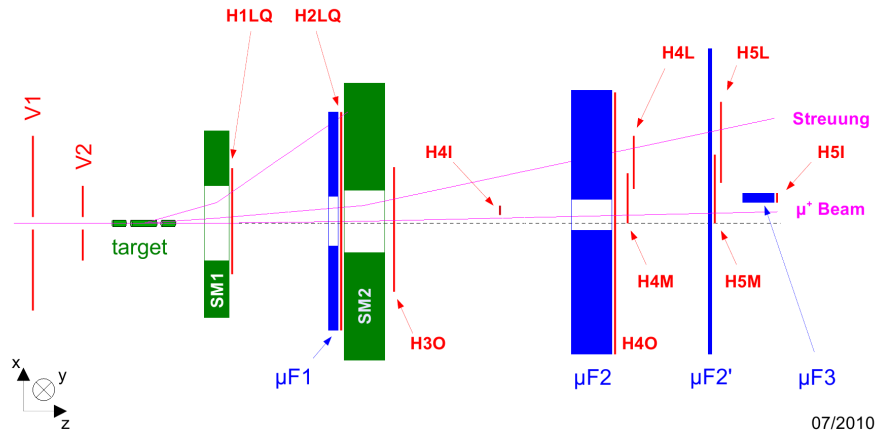


**Figure 5:** Trigger hodoscopes and veto detectors (both coloured red) of the COMPASS experiment. The hodoscopes are sorted into groups of two. [Bi10]

The trigger concept mainly follows one idea which is that only those events in which the outgoing particles' tracks pass the target region and do not belong to the halo beam are meaningful. Halo muons can be excluded by two veto detectors in front of the target around the beamline (compare fig. 5). If those veto detectors give out a signal it is clear that the corresponding events

include a halo muon and is therefore not stored. To check whether the outgoing particles have passed the target region the so called “target pointing” is applied. This is realised via several trigger hodoscopes and is coupled with the detection of an outgoing hadron in the HCAL. Only if the deposited energy of the detected hadron exceeds a certain threshold this event is considered meaningful. Detecting the outgoing hadrons  $K^-$  and  $\pi^+$ , the reaction in equation (4) can in be identified. The trigger hodoscopes each contain 16-32 strips so that they can, in combination with reading them out at both ends, provide a certain spacial resolution [Pr07].

If two of the trigger hodoscopes detect the same muon, target pointing can be checked. This is done via the trigger matrix shown in figure 6. Each scintillator strip has its own matrix element and it is checked whether the combination of the current two strips that have been passed by one muon fulfills the condition of target pointing. In the next step, whether the hadron energy threshold is exceeded is checked. If this is the case then a trigger signal is generated. In order to manage this the trigger hodoscopes are sorted in groups of two. Each of those groups covers a certain angular range, which can be seen in figure 5.

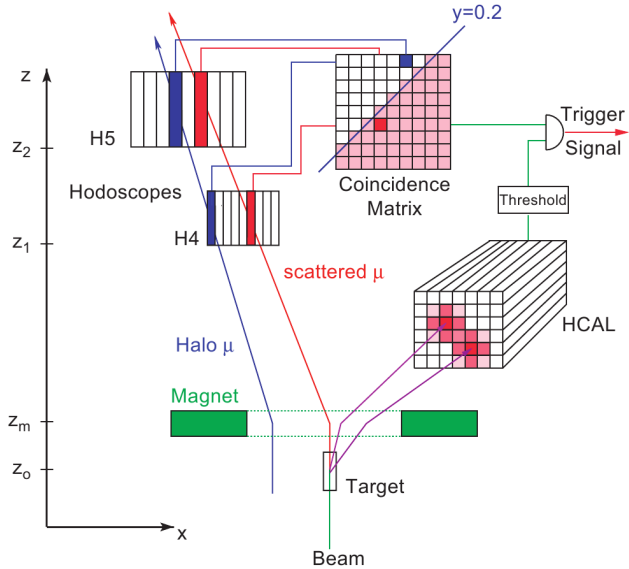


**Figure 6:** *Triggermatrix of the COMPASS trigger. [Ab07]*

### Origin of the histograms

The signals of the strips will not arrive at the same time at the matrix logic, due to the time that a muon needs to pass from the first to the second member of the hodoscope group and because of different cable runtimes (compare figure 6). The instant in time when the triggering signal is generated will be determined by the arrival of the second signal as indicated in figure 7. Based on this fact, the instant in time when the trigger signal is generated does not correspond to the instant of time when the output of the first detectors signal took place. One then needs to know which area in the evolving signal output of the first detector corresponds to the event that released the trigger. In figure 7 the signals of the two hodoscopes, which have been hit are shown. They both arrive at different times and the triggering signal is not given out until the second signal arrives at the logic unit. The time difference from the arrival of the first signal until the one of the second is called  $t_0$  and is needed to fully reconstruct an event. The automatization of the determination of  $t_0$  is the scope of this work. This quantity can be determined directly from the data.

In this case, the histogram of a single detector channel is observed where the single hits are plotted

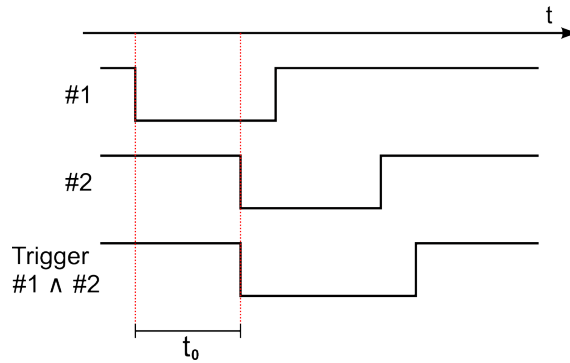


**Figure 7:** *Timing of the trigger signal and meaning of  $t_0$ .*

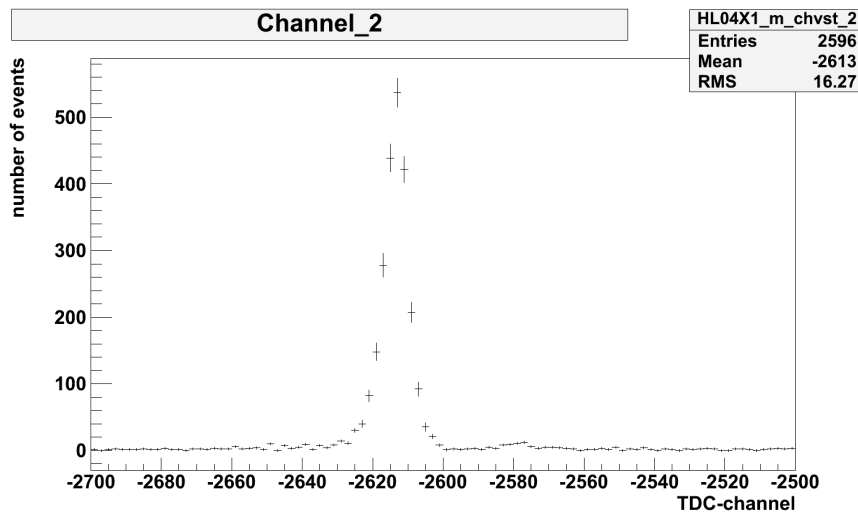


**Figure 8:** *Histogram with the data of one hodoscope channel from which the  $t_0$  can be determined.*

against the time difference to the triggering point of time. An example for such a histogram is shown in figure 8. At almost every point in time, a varying number of events can be found, but most events can be observed at one peak. The position of this peak in x-direction marks the size of  $t_0$ . So by determination of the peaks positions,  $t_0$  is known.

In a histogram, as can be seen in figure 8 the existing arbitrary time values of a measurement are grouped in x-intervals. These intervals are called bins where the number of events in each bin is counted and so the corresponding y-value is determined. The number of bins is usually set to 100 per histogram. The x-axis of the histograms corresponds to the *time to digital converter* (TDC) channels.

On the one hand a TDC can be used to create a reference point for the time of arrival of every incoming pulse or on the other hand to determine the time lag between two incoming signals. A TDC can't be used to measure a single time point because its channels can include arbitrary shift in time due to cable length and response time of electrical components. But when looking at the difference of two points in the histogram, this can be converted into a time difference with known units because each TDC-channel corresponds to a width of 108.3ps.

Because the histogram shows all events that entailed a triggering signal, of course this includes those cases where the observed hodoscope itself was responsible for the triggering point of time. In this case it leads to a self stopping peak, which is mostly narrow and can be observed in many histograms (for example in figure 16).

### 3 Automised determination of $t_0$ offsets using *ROOT*

The task of this work is to determine the  $t_0$  timing by fitting GAUSS-peaks to the different channels of the detectors. In the following the realisation of the  $t_0$  determination is described.

Although fitting is already implemented and automated in *ROOT*, there is no predefined function that is able to fit GAUSS-functions either with offset or with multiple peaks. The histograms show a mostly constant y-axis offset and some of them have additional peaks. Hence a function with the ability to describe multiple GAUSS-peaks with an offset is essential and has to be defined by the user. In this work the function is defined as follows

$$f(x) := y_0 + A_p \cdot e^{-\frac{(x-C_p)^2}{2 \cdot \sigma_p^2}} + A_s \cdot e^{-\frac{(x-C_s)^2}{2 \cdot \sigma_s^2}} \quad (6)$$

where  $y_0$  is the offset of the y-axis. The variables  $A_p$  and  $A_s$  stand for the amplitudes,  $C_p$  and  $C_s$  for the peaks' centers and  $\sigma_p$  and  $\sigma_s$  for the widths of the primary and the secondary peak respectively.

Due to the fact that this function has seven free parameters, these parameters need meaningful starting values to achieve good fitting results. Limiting the range of the parameters can also be an effective way of saving time during the fitting progress.

#### 3.1 General program layout

In the following the method of operation during one program call is explained. The program is started for one detector and then determines the  $t_0$ 's for all channels automatically by fitting the corresponding peaks. In order to make the user able to examine the quality of the fit very quickly, the histogram of each channel is plotted on a subcanvas with the applied fit and the resulting  $t_0$ . Finally the program has to write the  $t_0$ 's into a file that can be used to transfer them to the experiment. A general overview about the programs functionality can be found in figure 9.

#### 3.2 Implementation of fit

The first step that the program has to make is to recognise whether the current channel has one or two peaks. To achieve this, the program searches for the maximum of the current histogram and fits a first peak to it. For the search of potential secondary peaks the width of the first fitted peak is excluded and the next maximum is searched for in the rest of the histogram. To prevent the program from fitting the first peak too narrow, a lower boundary for the width is preset. Here the number of events in this channel influences the minimal allowed size of the width, assuming that a low number of events leads to broader GAUSS-peaks and that a large number of events leads to rather narrow peaks. After fitting the first peak the remaining parts of the histogram to the left and to the right of the peak are searched for the possible second peak. The distance from the peak centre that is excluded from search is determined by the condition that the peak should drop down to  $e^{-3}$  of its amplitude. After finding one candidate on each side of the peak, the higher of them is examined and it is checked, whether it exceeds five times the y-offset and, in case the y-offset is very small due to miscalculations, it has also to exceed the absolute value of three. If conditions are satisfied, a secondary peak is identified. The calculation of the y-offset will be discussed in the next paragraph.

As already mentioned in the case of seven fitting parameters in one function, it is mandatory to initialise them. The first parameter to determine is the y-offset of the histogram. An approximation of it is found, when calculating the mean y-value of the boundary bins, on both ends of the histogram. One each end of the histogram one takes into account the fifteenth part of the total number of bins. Out of these bins the average is calculated and so the starting value is fixed.

The amplitudes of both peaks, which have already been determined are set as starting values for the amplitudes of the peaks, which belong to the fit-function. Their position can be obtained by identifying the corresponding x-values which can then be set as the x-offset for the peaks. Additionally the widths of the peaks are adjusted to an expected value of 8ns.

In order to limit the needed time for fitting, it is sensible to limit the range of parameters to realistic values. In case of the amplitudes, we allow a range that goes from zero to ten times the previous defined maximal value of the histogram. For the peak centres only the range of the histogram is allowed. In addition to that the allowed range for the y-offset is from zero to 10 times its previous approximation.

Having set the parameters boundaries the fit now can be applied. So either the full GAUSS-function of equation (6) is plotted or the parameters  $A_s$ ,  $C_s$  and  $\sigma_s$  are fixed at zero. Of course this depends on whether the program detected one or two peaks. To achieve a higher accuracy, the fitting procedure is done several times until either there is no significant enhancement in the  $\chi^2$  value or the number of fits has reached five.  $\chi^2$  gives a degree of the consistency between the data and the fitted function and is automatically determined by the fitting procedure. The outcome of the fits is then plotted together with the corresponding data in the current subcanvas. The visible corresponding error is necessary for the fitting and has been rated to  $\sqrt{N}$ , where  $N$  is the number of events in one bin. Finally the  $t_0$  has to be determined and written to a file that can be read by the Data Acquisition (DAQ) software. If the program only finds one peak, the center of this peak is the  $t_0$ . If on the other hand the program detects two peaks, one of them has to be chosen. In general one expects that the peak which corresponds to  $t_0$  is broader than for example a self stopping peak. But in order to prevent the software from choosing the secondary peak with lower amplitude that may have a very big width but describes the background, we require that two conditions are fulfilled. Firstly, the amplitude of the secondary peak should be at least 60% of one of the primary amplitudes and, secondly, its amplitude should be greater than 30% of the maximal value of the histogram. If these conditions are not satisfied by the secondary peak, the first one is chosen to be the  $t_0$ -peak. This result is then written to a ".dat" file named after the detector including a line for each channel with the corresponding  $t_0$ -time.

For effective evaluation of  $t_0$  determination, a vertical line is plotted in the corresponding histogram at the chosen  $t_0$  position. So the user can quickly check whether the fit worked well and whether  $t_0$  was determined correctly. For further information, the program code can be found in the appendix.

Although it was planned to design the program with data from the 2011 run, this couldn't be realised because in the beamline from SPS to COMPASS some parts which are essential for beam delivery to COMPASS, broke. For this reason I was unable to obtain data during my stay at CERN. Therefore the program was designed and developed with data recorded in september 2009, from the file "trigtime\_79628.root". In the next section the results of this implementation can be found.

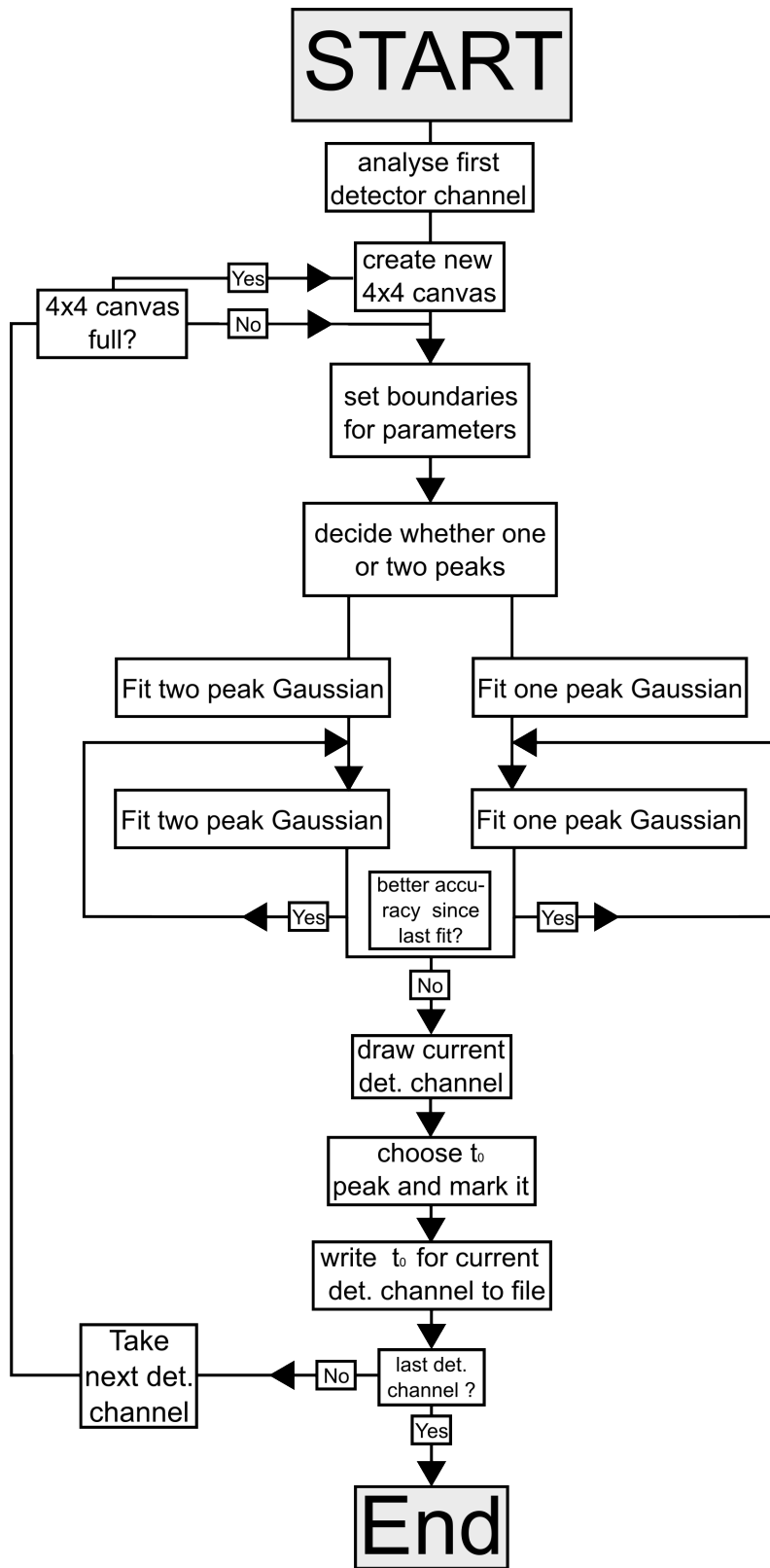
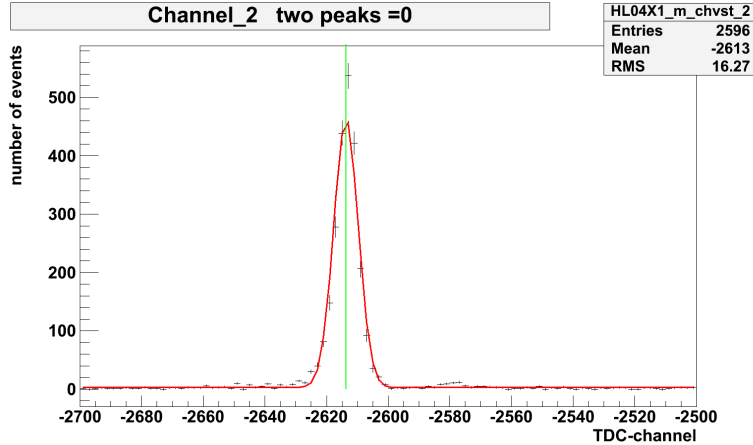


Figure 9: General functionality of the program.

## 4 Results

In this section, the results of the fitting progress will be presented. Firstly some fitting results will be presented and discussed. Secondly to demonstrate the approach to the task described in chapter 3, the mode of operation of three subroutines including their results will be presented.

In order to evaluate the quality of the fits and the determination of the  $t_0$ , some histograms with



**Figure 10:** Good single peak fit result for channel 2 of detector data *HL04X1\_m\_chvst*. The green line marks the position of the peak associated to  $t_0$  by the program.

good and bad results will be presented and discussed. A rather simple task for the program is to fit a single peak, like in figure 10, which works in all cases that have been tested. In some cases a low number of events inhibits correct fitting results as shown in figure 11.

In this case the reason for the bad result might be the fact that the histogram has two maximal values with identical height. As the program can only store one maximal value, the left one will probably be taken and therefore the first fit is initialised with this x-axis offset. This leads to the result pictured in figure 11. Otherwise, in most cases low statistic needn't imply bad fit results as indicated in figure 12.

Many histograms include secondary peaks, which have to be discovered by the program and

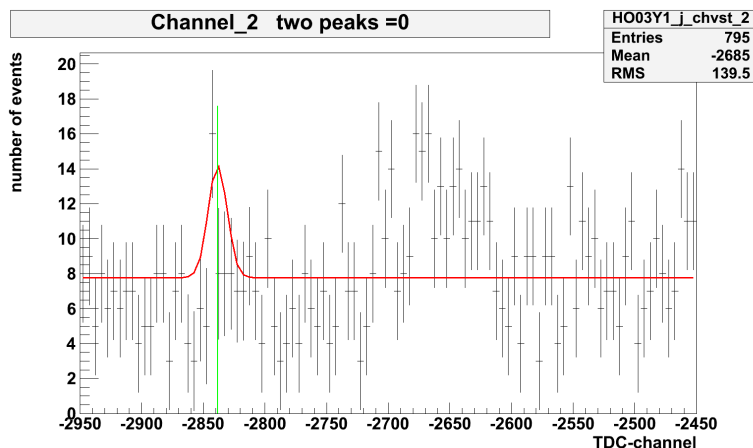


**Figure 11:** bad fit result because of the low number of events. The green line marks the position of the peak associated to  $t_0$  by the program.

correctly fitted. The determination of  $t_0$ , is achieved in nearly all cases, but in some cases secondary peaks are not detected as can be seen in figure 13. In this case it is due to the condition that needs to be fulfilled in order to identify a second peak. In order to detect the secondary peak,

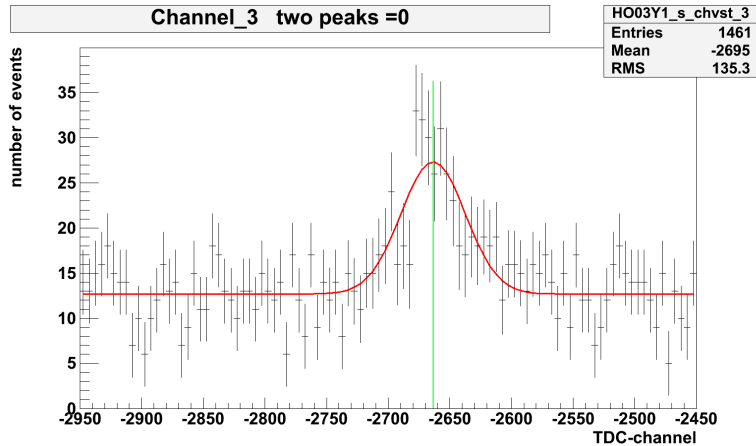


**Figure 12:** good fit result although the low number of events. The green line marks the position of the peak associated to  $t_0$  by the program.

its amplitude (here 41) needs to be larger than five times the y-offset, which is in this case 9.58, and the amplitude has to exceed the total value of three. So this condition is not fulfilled and the peak is not found. These conditions have been optimised to fit most of the histograms but cannot cope with all of them. An example where these conditions are well suited can be seen in figure 14.

During the design of the fitting procedure, several problems occurred whose solution led to new

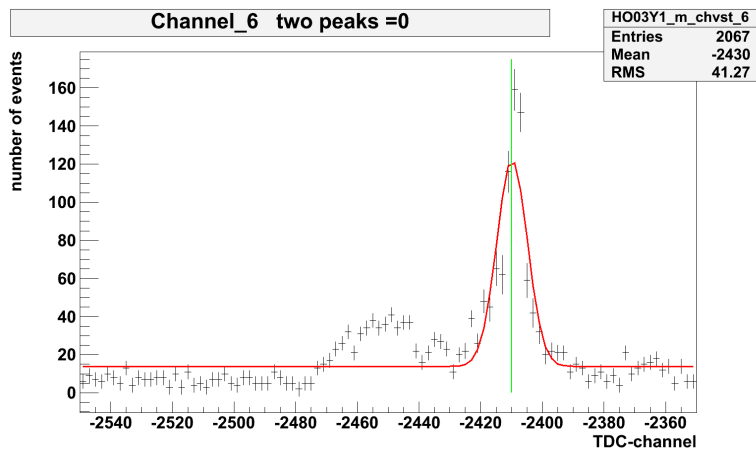


**Figure 13:** Although  $t_0$  has been determined correctly in this fit, the second peak of the histogram couldn't be found by the program. The green line marks the position of the peak associated to  $t_0$  by the program.

subroutines of the program. To demonstrate the functionality of those subroutines, the histograms of some of the problematic channels are shown both with switched off and working subroutine.

### subroutine minimal width

As already mentioned, the program searches for the maximal value of the whole histogram to have a starting value for the peak position. In some cases the program tries to fit a very narrow peak around this maximum, which does not fit to the data but describes the statistical fluctuation like in figure 15 part (a). This is the case particularly for histograms with a low number of events. When the histogram does have less than 1500 events, the minimal allowed width is set to 45ns and for histograms with more entries to 20ns. As result of this constraint, the program fits broader

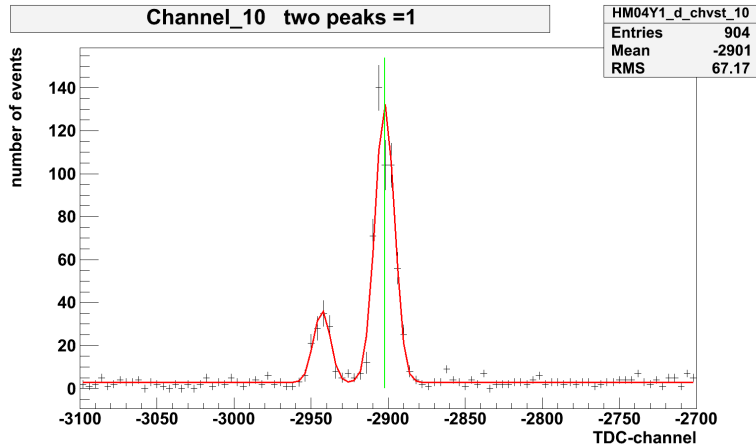


**Figure 14:** *Fit with correctly determined secondary peak out of hodoscope HM04Y1\_d\_chvst. The green line marks the position of the peak associated to  $t_0$  by the program.*

peaks and is therefore able to describe the data more correctly as it can be seen in the part (b) of the figure.

#### subroutine search intervall

Before searching for a second peak a first fit with one peak is applied in order to exclude its range from the interval to be scanned for the second peak. Without including a second peak the program only tries to fit one peak to the whole histogram, which cannot describe the data properly (compare part (a) of figure 16). So the remaining part of the histogram is scanned for a second peak and it can be identified. If a second peak is found, the complete GAUSS-function from equation (6) is fitted and the histogram can be described well. In the part (b) of figure 16 the search intervall subroutine is included.

#### subroutine multiple fits

In order to achieve good agreement between data and fit, the main fitting procedure is done several times until the new fit does not converge better than the last one or the total number of fits done at this point has reached five. It is meaningful to give a weighting of the datapoints to the fitting procedure, so their errors are set to the satistical error of  $\sqrt{N}$  where  $N$  is the number of events. This leads to a better description of the data which can be seen in figure 17. In this case the y-offset is described better.

To summarise, the program works well for the 2009 data, for which it has been optimised. From about 300 channels which are included in the data of “trigtime\_79628.root” in only four cases the  $t_0$  determination couldn’t be achieved automatically by the program. Examples for the program output can be seen for a complete detector each in figure 18 and 18.

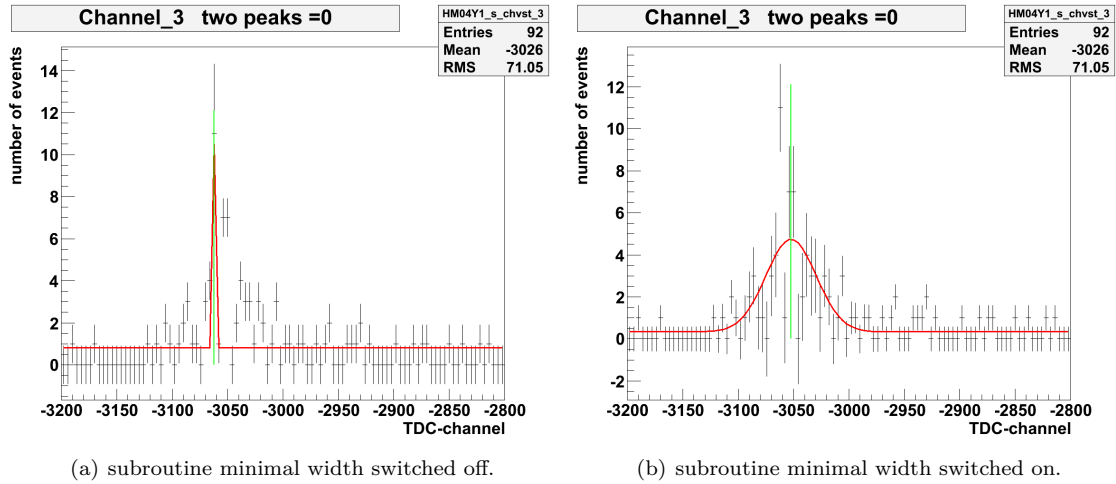


**Figure 15:** Demonstration of the minimal width functionality of the program using the example of channel 3 of the *HM04Y1\_s\_chvst* detector data. The two different variants of fits are applied to the same amount of data. The green lines mark the position of the peaks associated to  $t_0$  by the program.

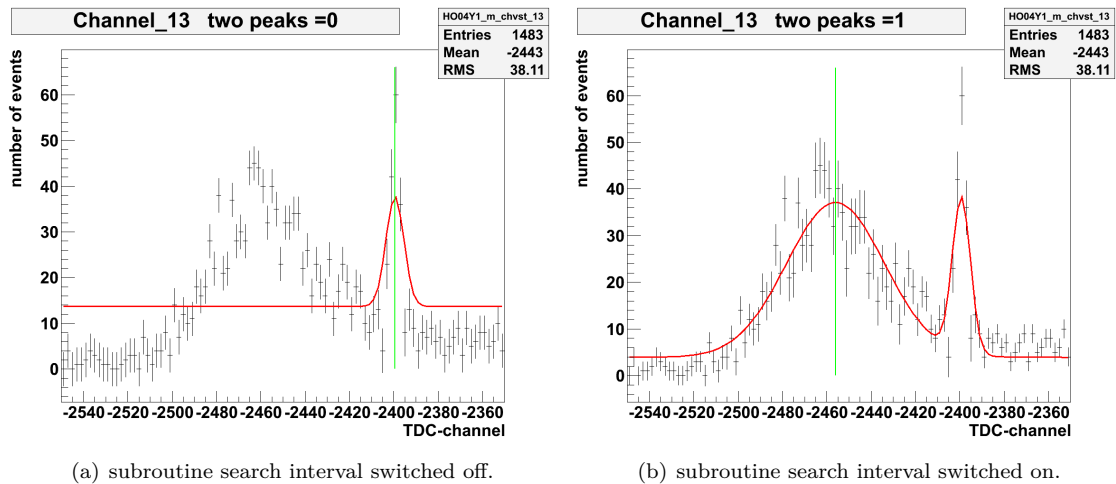
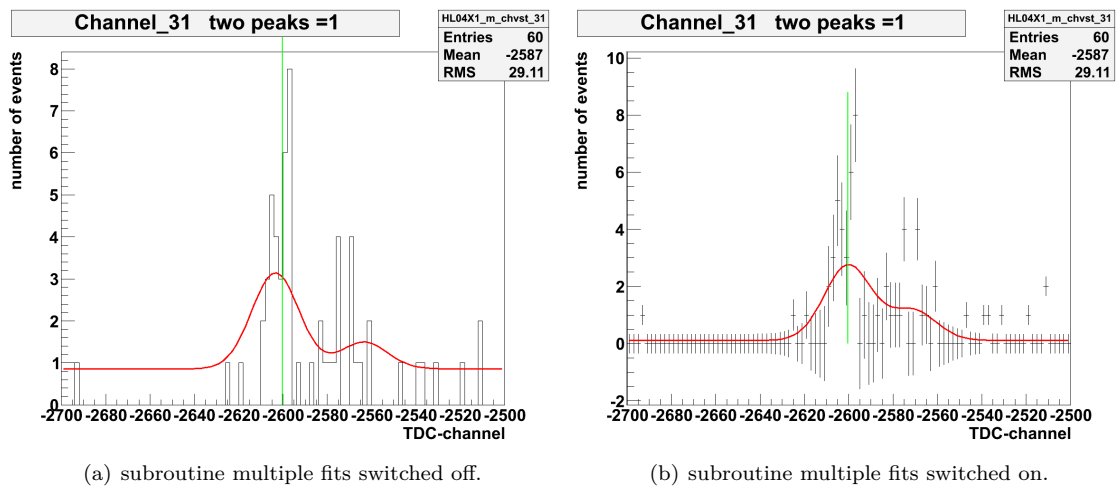


**Figure 16:** Demonstration of the search interval functionality of the program using the example of channel 3 of the *HO04Y1\_m\_chvst* detector data. The two different variants of fits are applied to the same amount of data. The green lines mark the position of the peaks associated to  $t_0$  by the program. On the right side of the main peak a self stopping peak can be observed.



(a) subroutine multiple fits switched off.

(b) subroutine multiple fits switched on.

**Figure 17:** Demonstration of the multiple fits functionality of the program using the example of channel 31 of the HL04X1\_m\_chvst detector data. The two different variants of fits are applied to the same amount of data. The green lines mark the position of the peaks associated to  $t_0$  by the program.

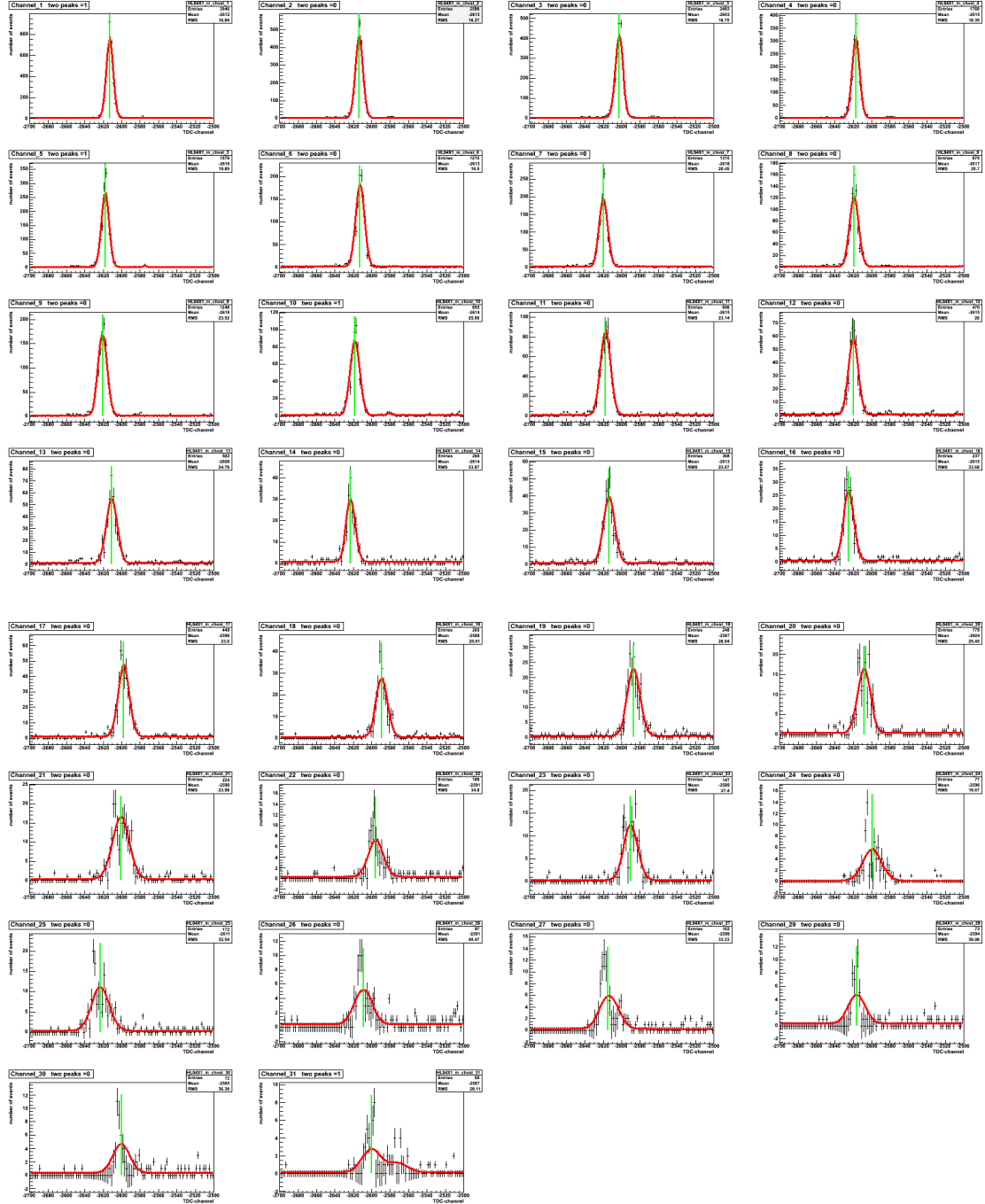


Figure 18: Example for the complete HL04X1\_m\_chvst detector data with applied fits and determined  $t_0$ 's.

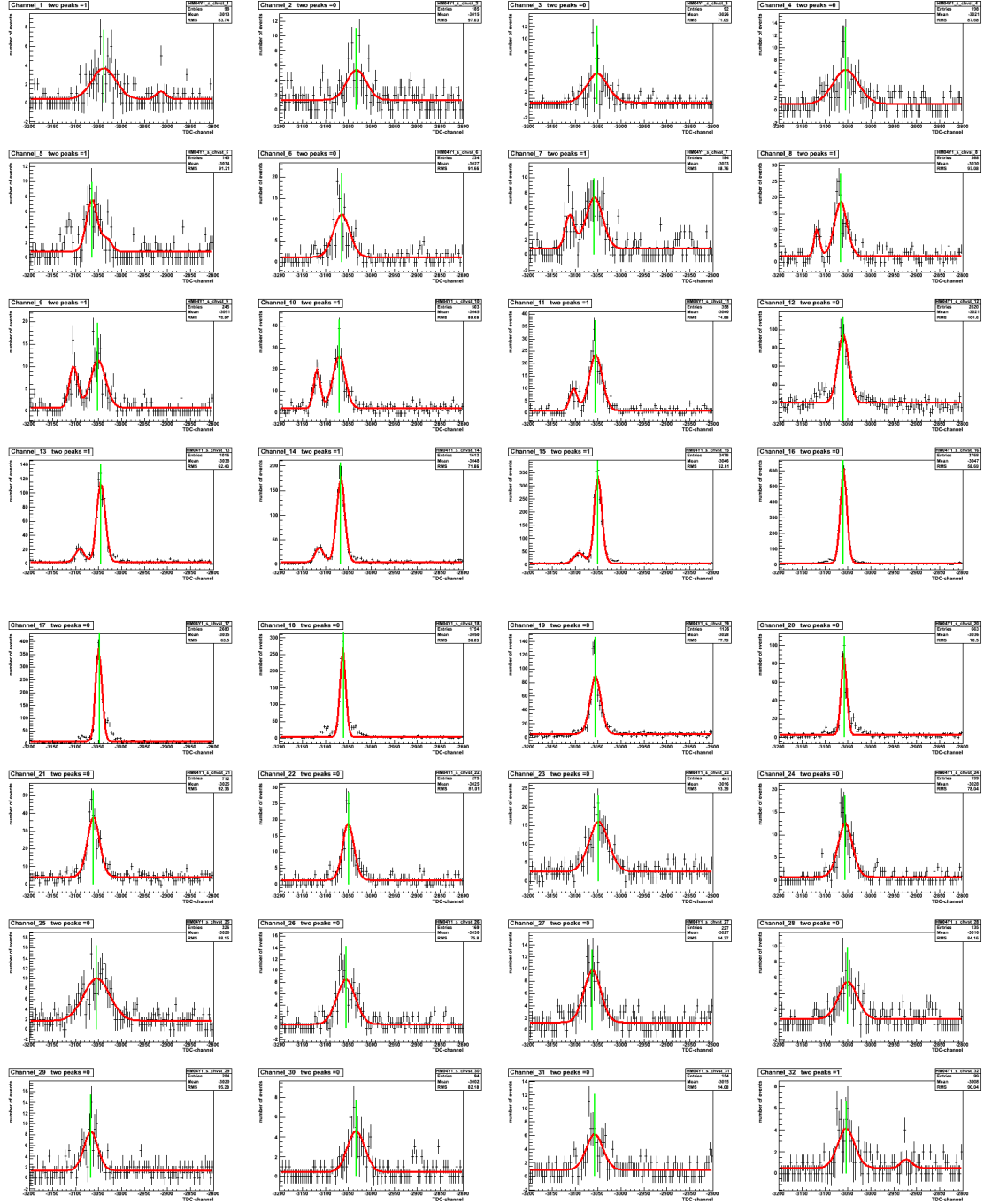


Figure 19: Example for the complete HM04Y1\_s\_chvst detector data with applied fits and determined  $t_0$ 's.

## 5 Summary and outlook

The COMPASS experiment aims to measure among other things the gluon spin contribution to the nucleon spin. Its core is a two stage spectrometer, designed to cover a broad momentum acceptance. The two spectrometers include several hodoscopes which are responsible for the trigger. In order to get the trigger timing for the hodoscopes, the previously described *ROOT* program was written. For this scope the program is called for one detector and then analyses each channel of this detector automatically. It fits a GAUSS-function with offset and two peaks to those spectra where more than one peak can be found and only one in the other case. After fitting the function, the peak that identifies  $t_0$  is selected and marked in the output histograms. In these histograms the single channels are plotted in order to enable the user to quickly check the  $t_0$  determinations. After the program is finished, a file named after the detector is created. In this file the trigger timings for the channels of the detector are written down, so that they can directly be used for the experiment.

The results for the “trigtime\_79628.root” data from 2009 are good. For nearly all of the 300 included channels the  $t_0$  is determined correctly. The secondary peaks are found in most cases, if they differ clearly from the offset.

Due to the damage at the beam feed in, the new trigger file from 2011 arrived just a few days before the end of this work. Inspecting the new data, it turns out that the included data channels offer a quite different shape. In particular the new data offers higher statistics and includes the existence of many triple peaks, which couldn't be observed in the old file. So as a future prospect the program can be optimised for the new circumstances of the 2011 data.

The program can be found on the following web page:

[http://hsag.physik.uni-bonn.de/docs/public/rossbach/t0\\_fit\\_ver6.C](http://hsag.physik.uni-bonn.de/docs/public/rossbach/t0_fit_ver6.C)

## References

- [Ab61] A. ABRAGAM, *The Principles of Nuclear Magnetism*, The Clarendon Press, Oxford (1961).
- [Ab07] P. ABBON ET AL., *The COMPASS experiment at CERN*, Nucl. Instr. and Meth. Phys. Res.A 577(2007), p. 455.
- [As88] J.ASHMAN ET AL., *A measurement of the spin asymmetry and determination of the structure function  $g_1$  in deep inelastic muon-neutron scattering*, Phys. Lett.B 206(1988), p. 364.
- [Be05] C. BERNET ET AL., *The COMPASS trigger system for muon scattering*, Nucl. Instr. and Meth. Phys. Res.A 550(2005), p. 217.
- [Bi10] JOHN BIELING, *Entwicklung eines ungetakteten 64-Kanal-Meantimers und einer Koinzidenzschaltung auf einem FPGA*, Diplomarbeit, Bonn 2010.
- [CE08] <http://te-epc-lpc.web.cern.ch/te-epc-lpc/machines/pagesources/Cern-Accelerator-Complex.jpg>
- [He09] ROMAN HERMANN, *Die Messung der Gluonpolarisation durch die Produktion von Hadronenpaaren mit großen Transversalimpulsen in tieflinelastischen Myonstreuung am Nukleon*, Dissertation, Mainz 2009.
- [Po09] BOGDAN POVH ET AL., *Teilchen und Kerne - Eine Einführung in die physikalischen Konzepte*, Springer-Verlag, Berlin Heidelberg (2009).
- [Pr07] JÖRG PRETZ, *The Gluon Polarization in the Nucleon from the COMPASS Experiment*, Habilitationsschrift, Bonn 2007.